FINITE ELEMENT SIMULATION OF SHAPE MEMORY COUPLINGS

Leonardo Boselli da Motta
Dianne Magalhães Viana
Edgar Nobuo Mamiya
Universidade de Brasília, Faculdade de Tecnologia, Departamento de Engenharia Mecânica, 70910-900 Brasília, DF, Brasil. E-mail: boselli@lion.enm.unb.br

Abstract
Hydraulic tube couplings for jet fighters can be fabricated from NiTi alloys. The use of NiTi alloys is an alternative of the difficult task of brazing hydraulic lines. In this case, the NiTi sleeve is mechanically expanded at low temperature, then placed around the tubes to be joined. In the sequence, it is warmed up to room temperature, when it recovers its original shape, gripping firmly the tubes. The goal of this paper is to present a qualitative finite element analysis of such pipe coumpling.

Keywords: shape memory, pipe coupling, finite element.

1. INTRODUCTION

Shape memory alloys (SMAs) are materials which, after being subjected to a severe inelastic deformation, can recover its original shape whenever it undergoes an appropriate increase of temperature. Such unique mechanical behavior is associated with stress-induced phase transformations from twinned martensite to detwinned martensite (during inelastic deformation) and from detwinned martensite to austenite (during shape recovery). Representative materials exhibiting shape memory include NiTi, CuZnAl, CuAlNi, AuCd alloys. Since the early sixties this class of materials has been considered for the design of pipe couplings, fasteners, clamps, "smart" structures, advanced composites, force actuators and heat engines. Shape memory alloys have been succesfully employed to couple hydraulic-fluid lines in jet fighters as an alternative to the difficult task of brazing lines that lie close to the aluminum skin: a NiTi sleeve is expanded in the martensitic condition at liquid nitrogen temperature, then placed around the tubes to be joined; during warming to room temperature, the sleeve recovers its original shape, producing a tight seal. The use of such fittings avoids metallurgical degradation which can result from welding or brazing, and avoids damage to the aircraft skin. Over 300,000 such high performance connectors have been used in US Navy aircrafts with no reports of failures (Wayman, C. M. (1980)).

Many models have been proposed for the description of the thermomechanical behavior of shape memory alloys, including those reported by Graesser & Cozarelli (1994), Leclercq & Lexcellent (1996), Auricchio & Taylor (1997) and Souza et al. (1998), amongst many others. One interesting feature of the model proposed by Souza et al. is the fact that it showed a satisfactory qualitative agreement with experimental data (Sittner et al. (1995)) when nonproportional load histories were applied to the material. This feature is welcome in the setting of a finite element code, where very general load histories are expected.

The goal of this paper is to present some numerical results related to the development

of a finite element capable to describe the thermomechanical behavior of shape memory alloys, as described by Souza et al.. In particular, we present a simulation of the assembling process of a jet pipe coupling.

2. THE MECHANICAL MODEL

If ε denotes the classical *linear strain* tensor, then the corresponding *deviatoric strain* tensor is defined as $\mathbf{e} := \varepsilon - \frac{1}{3}(tr\,\varepsilon)\,\mathbf{I}$, where $\mathbf{I}$ is the identity tensor in R^3. If $\mathbf{T}$ denotes the Cauchy stress tensor, then the *deviatoric stress* tensor $\mathbf{S}$, work-conjugate to $\mathbf{e}$, is given by $\mathbf{S} := \mathbf{T} - \frac{1}{3}(tr\,\mathbf{T})\,\mathbf{I}$. A symmetric and deviatoric *transformation strain* $\mathbf{e}_T$ describes the average detwinning (and hence the phase transformation) in the material. When $\mathbf{e}_T = \mathbf{0}$, we say that the material is in its parent phase (austenite or twinned martensite), when $||\mathbf{e}_T|| = \xi_s$, the material is in its product phase (detwinned martensite), and when $0 < ||\mathbf{e}_T|| < \xi_s$ a mixture of both parent and product phases can be observed in the material.

Souza et al. proposed two potentials from which the constitutive relations and the evolution law for the transformation strain $\mathbf{e}_T$ are derived. The first potential is the *Helmholtz free energy*:

$$\psi(tr\,\varepsilon, \mathbf{e}, \mathbf{e}_T, \theta) := \left(\frac{\lambda}{2} + \frac{\mu}{3}\right)(tr\,\varepsilon)^2 + \mu\,||\mathbf{e} - \mathbf{e}_T||^2 + \tau_M(\theta)\,||\mathbf{e}_T|| \tag{1}$$

where λ and μ are the Lamé constants of the material and $\tau_M(\theta)$, a positive and monotonically increasing function of the temperature θ, is the so called Maxwell stress (see Gurtin (1983), for instance). Differentiation of the potential Ψ with respect to state variables gives the following constitutive relations:

$$T_m := \frac{\partial \psi}{\partial (tr\,\varepsilon)}(tr\,\varepsilon, \mathbf{e}, \mathbf{e}_T, \theta) = \left(\lambda + \frac{2\mu}{3}\right) tr\,\varepsilon, \tag{2}$$

$$\mathbf{S} := \frac{\partial \psi}{\partial \mathbf{e}}(tr\,\varepsilon, \mathbf{e}, \mathbf{e}_T, \theta) = 2\mu\,(\mathbf{e} - \mathbf{e}_T), \tag{3}$$

$$\mathbf{X} \in -\partial_{\mathbf{e}_T}\psi(tr\,\varepsilon, \mathbf{e}, \mathbf{e}_T, \theta) = \mathbf{S} - \tau_M(\theta)\,\partial\,||\mathbf{e}_T||, \tag{4}$$

$$\eta \in -\partial_\theta\,\psi(tr\,\varepsilon, \mathbf{e}, \mathbf{e}_T, \theta) = -\partial\,\tau_M(\theta)\,||\mathbf{e}_T||. \tag{5}$$

Equation (2) describes the mean stress corresponding to changes in the volume of the material while equation (3) is the deviatoric stress-strain relation. The *transformation stress* $\mathbf{X}$, work-conjugate to the transformation strain $\mathbf{e}_T$, is the driving force for phase transformation processes. The term $\tau_M(\theta)\,\partial||\mathbf{e}_T||$ describes the "origin" of the elastic domain. Finally, η is the density of entropy.

The second potential considered in the model is the *complementary potential of dissipation* ϕ^c, defined as:

$$\phi^c(\mathbf{X}) = I_R(\mathbf{X}) := \begin{cases} 0 & \text{if } ||\mathbf{X}|| \le R, \\ +\infty & \text{otherwise.} \end{cases} \tag{6}$$

Differentiation of (6) with respect to $\mathbf{X}$ leads to the following *flow rule*:

$$\dot{\mathbf{e}}_T \in \partial\,\phi^c(\mathbf{X}) = \partial\,I_R(\mathbf{X}). \tag{7}$$

An Implicit Euler scheme, together with a classical Return Mapping Algorithm, was considered for the integration of the aforementioned flow rule. Further details can be found in Souza et al. (1998).

3. FINITE ELEMENT SIMULATION OF HYDRAULIC COUPLINGS

In this section we present a numerical simulation of the assembling process of a Nitinol hydraulic coupling. In this setting, let us consider a pair of aluminum tubes with inner and outer diameters $\phi_i = 6\ mm$ and $\phi_o = 12\ mm$, respectively. A shape memory sleeve with inner and outer diameters $\Phi_i = 11.52\ mm$ and $\Phi_o = 18\ mm$, respectively, is machined at room temperature, so that the inner diameter of the sleeve is about 4% less than the outer diameter of the tubes (Fig. 1.a). The sleeve is then cooled up to $-120°C$ and mechanically expanded to have an inner diameter 4% larger than the tube's outer diameter (Fig.1.b). Still at low temperature, the set is assembled (Fig. 1.c). When the couple is warmed up to room temperature, it shrinks to form a tight seal (Fig. 1.d).

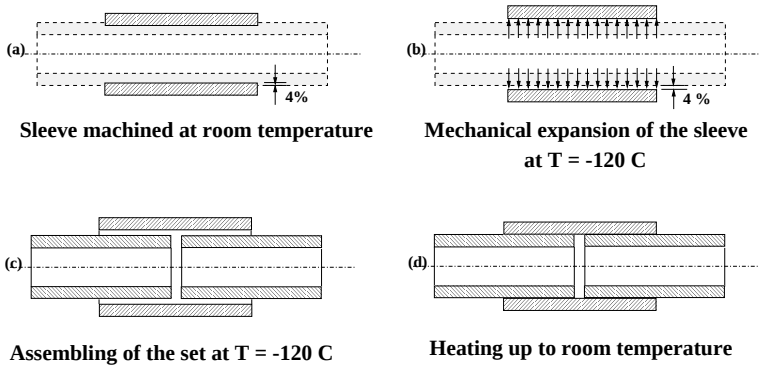

Figure 1: Schematic assembling process of the SMA coupling.

In order to simulate the aforementioned coupling process, two finite element discretizations were considered. The first one is illustrated in Figure 2 and considers that the problem is invariant along the longitudinal direction. As a consequence, the discretization is restricted to the radial direction. The aluminum tubes are discretized in four elastic four-noded axisymmetric elements, while the sleeve is discretized in four shape memory four-noded $\bar{\mathrm{B}}$ axisymmetric elements. $\bar{\mathrm{B}}$ elements were chosen in order to avoid the locking associated with the evolution of the transformation strain, which is a deviatoric tensor. Two simple "gap" elements are considered in order to describe the contact condition between the sleeve and the tubes.

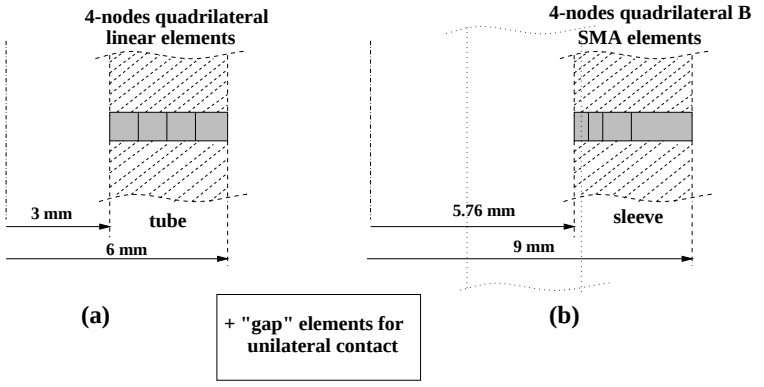

Figure 2: Discretization of the coupling along the radial direction: (a) tubes, (b) sleeve.

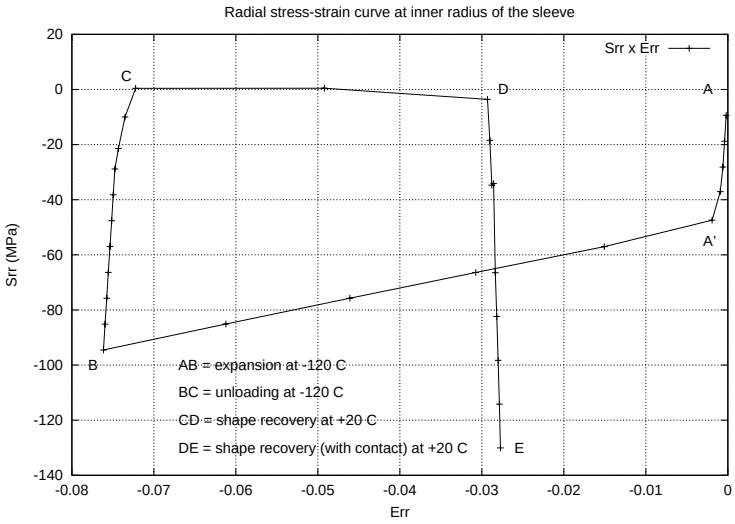

Figure 3: Radial stress-strain curve at inner radius of the sleeve.

Figure 3 describes the history of radial stress versus radial strain, at the inner radius of the sleeve, obtained from the numerical simulation of the assembling process. Starting from a stress-free configuration (at temperature $-120°C$), elastic behavior is observed from point A to point A', during mechanical expansion of the sleeve . Still during mechanical expansion, inelastic behavior associated with stress induced phase transformation is observed along line A'B. Line BC describes the stress-strain curve during unloading, always at cryogenic temperature. Next, line CDE is associated with elevation of the temperature up to $20°C$. Contact between the sleeve and the tubes starts at point D, as a consequence of the shape recovery of the sleeve.

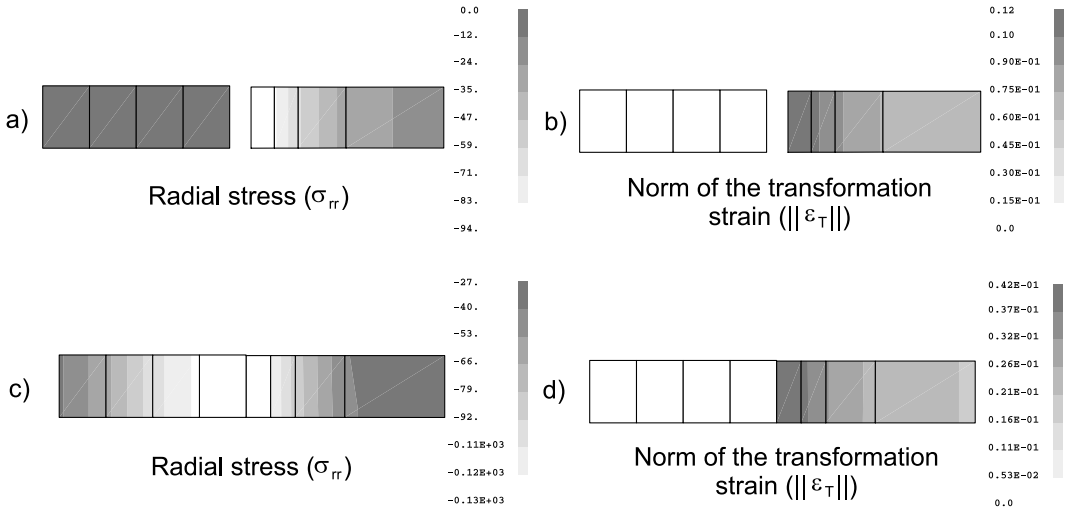

Figure 4: (a) Distribution of radial stress when maximum radial expansion of the sleeve is attained; (b) Distribution of $||\mathbf{e}_T||$ when maximum radial expansion of the sleeve is attained; (c) Distribution of radial stress after shape recovery of the sleeve; (d) Distribution of $||\mathbf{e}_T||$ after shape recovery of the sleeve.

Figure 4 describes the distributions of radial stress and of norm $||\mathbf{e}_T||$ of the transformation strain on the coupling at two distinct stages: when maximum radial expansion of the sleeve is attained (Figures 4.a and 4.b) and after shape recovery of the sleeve (Figures 4.c and 4.d). It is interesting to observe from Figure 4.d that, after shape recovery, the martensitic phase is still present in the coupling ($||\mathbf{e}_T|| > 0$). As a consequence, the sleeve can undergoe a further shape recovery even if small variations of the outer diameter of the tubes are observed.

The second discretization is illustrated in Figure 5 and consists of partitions of the tubes in 40 elastic four-noded axisymmetric elements each, and of the sleeve in 81 shape memory four-noded $\bar{\mathrm{B}}$ axisymmetric elements. 28 "gap" elements were considered for unilateral contact between tubes and sleeve.

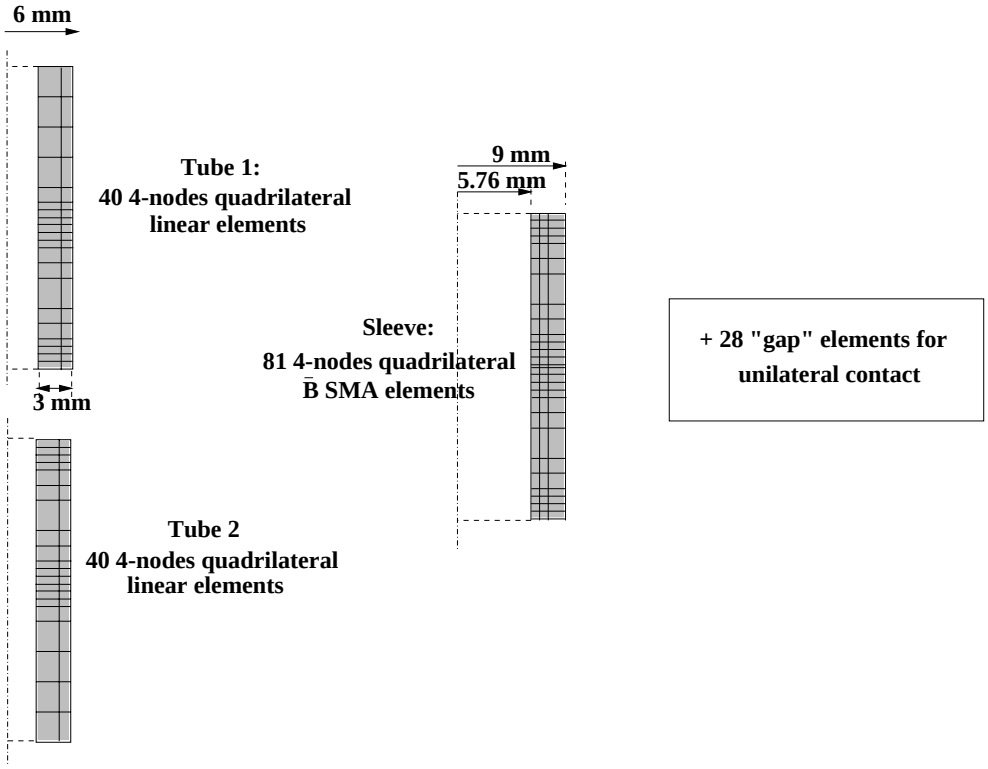

Figure 5: Second discretization of the coupling: partition of each tube in 40 elements and of the sleeve in 81 elements.

Figure 6 shows the corresponding distributions of the radial stress and of the norm $||\mathbf{e}_T||$ of the transformation strain on the coupling at two distinct stages: when maximum radial expansion of the sleeve is attained (Figures 6.a and 6.b) and after shape recovery of the sleeve (Figures 6.c and 6.d). Small differences of the results are observed when compared with those from the first discretization.

4. CONCLUDING REMARKS

The finite element discretization of the quasi-static evolution problem of a shape memory pipe coupling resulted in a set of nonlinear equations. Although a finite difference scheme was considered for the evaluation of the constitutive tangent moduli, quadratic convergence was observed during each isothermic step. The reasons for lower convergence rates associated with conditions of change in the temperature are under investigation.

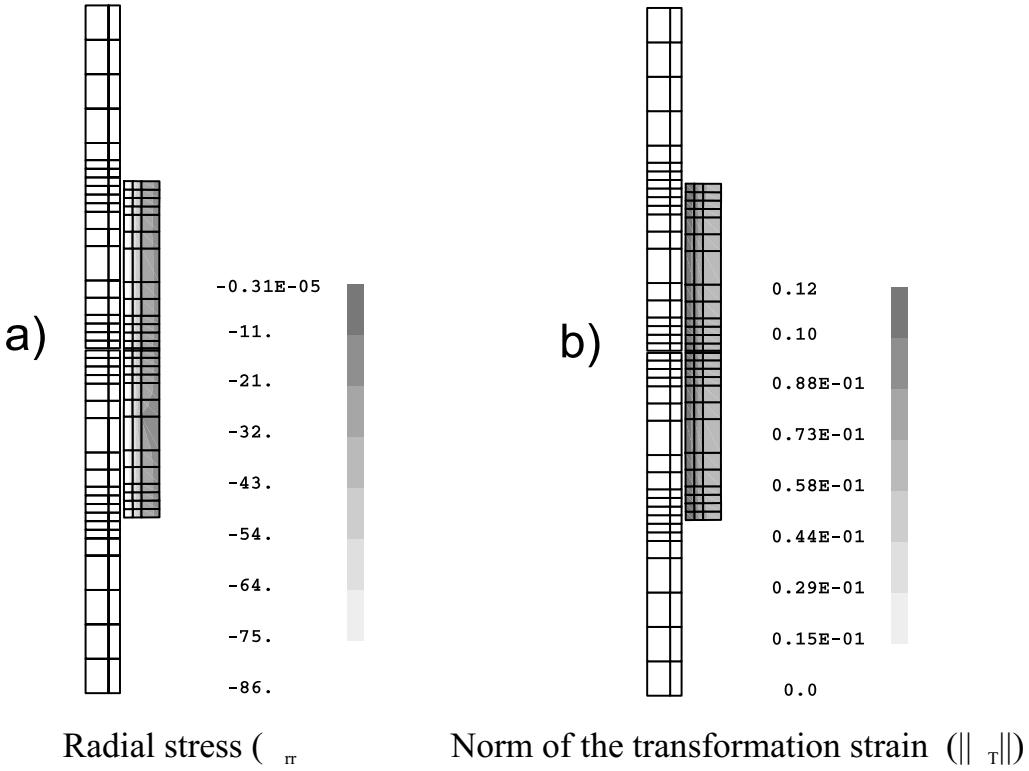

Radial stress ($_{rr}$ Norm of the transformation strain ($\| \ _{T}\|$)

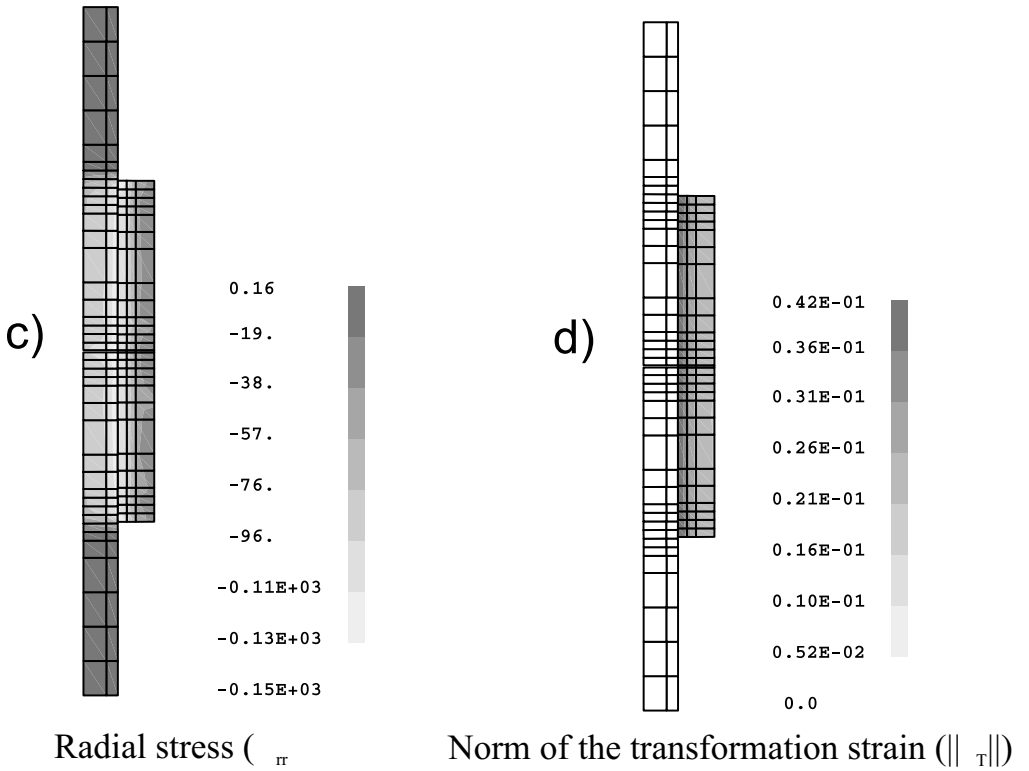

Radial stress ($_{rr}$ Norm of the transformation strain ($\| \ _{T}\|$)

Figure 6: (a) Distribution of radial stress when maximum radial expansion of the sleeve is attained; (b) Distribution of $||\mathbf{e}_T||$ when maximum radial expansion of the sleeve is attained; (c) Distribution of radial stress after shape recovery of the sleeve; (d) Distribution of $||\mathbf{e}_T||$ after shape recovery of the sleeve.

REFERENCES

- Auricchio F., Taylor R. L., 1997, "Shape-memory alloys: modelling and numerical simulation of the finite-strain superelastic behavior", Comp. Meth. Appl. Mech. Engrg., 143:175–194.

- Graesser E. J., Cozzarelli F. A., 1994, "A proposed three-dimensional constitutive model for shape memory alloys", J. Int. Mat. Systems and Structures, 5:78–89.

- Gurtin M. E., 1983, "Two-phase deformations of elastic solids", Arch. Rat. Mech. Anal., 84:1–29.

- Leclercq S., Lexcellent C., 1996, "A general macroscopic description of the thermomechanical behavior of shape memory alloys", J. Mech. Phys. Solids, 44:953–980.

- Sittner P., Hara Y., Tokuda M., 1995, "Experimental study on the thermoelastic martensitic transformation in shape memory alloy polycrystal induced by combined external forces", Metall. Mater. Trans. A, 26A:2923–2935.

- Souza, A. C., Mamiya, E. N., Zouain, N., 1998, "Three-dimensional model for solids undergoing stress-induced phase transformations", European Journal of Mechanics A/Solids, 17:789-806.

- Wayman, C. M., 1980, "Some applications of shape memory alloys", Journal of Metalls, 32:129–137.